Electronic Supplementary Information

A particulate photocathode composed of $(ZnSe)_{0.85}(CuIn_{0.7}Ga_{0.3}Se_2)_{0.15}$ synthesized with Na_2S for enhanced sunlight-driven hydrogen evolution

Yosuke Kageshima,[a] Tsutomu Minegishi,[ab] Yosuke Goto, ‡ [a] Hiroyuki Kaneko,[a] and Kazunari Domen*[a]

[a]Department of Chemical System Engineering, The University of Tokyo, 7-3-1 Hongo, Bunkyo-ku, Tokyo 113-8656, Japan. E-mail: domen@chemsys.t.u-tokyo.ac.jp

[b]Japan Science and Technology Agency/Precursory Research for Embryonic Science and Technology (JST/PRESTO), 7-3-1 Hongo, Bunkyo-ku, Tokyo 113-8656, Japan.

‡ Present address: Department of Physics, Tokyo Metropolitan University, Hachioji, Tokyo 192-0397 (Japan).

Optimization for calcination time of $(ZnSe)_{0.85}(CuIn_{0.7}Ga_{0.3}Se_2)_{0.15}$ particles

40% Cu-excessive particulate solid solutions of ZnSe and $CuIn_{0.7}Ga_{0.3}Se_2$, $(ZnSe)_{0.85}(CIGS)_{0.15}$, were synthesized by the flux method in a sealed quartz ampoule for various times, 10, 15, 40, and 80 h, in order to optimize calcination duration. All diffraction peaks in the XRD patterns (see Fig. S1a) of the specimens can be assigned to a zincblende phase, indicating the successful formation of solid solution of ZnSe and CIGS, regardless of the calcination time. They showed similar extent of crystallinity. The 40% Cu-excessive $(ZnSe)_{0.85}(CIGS)_{0.15}$ particles synthesized for various times showed absorption edge of around ~800 nm, and the weak light absorption at longer wavelength region over 800 nm (see Fig. S1b). The synthesis time did not affect the optical properties of the obtained particles, either. It was observed that the 40% Cu-excessive $(ZnSe)_{0.85}(CIGS)_{0.15}$ particles synthesized for various times possessed an indefinite and rugged shape, whereas their average particle size became larger according to the synthesis time (see Fig. S2). In the case of calcination time longer than 40 h, quite large particles with larger than 5—10 μm in diameter were observed.

The photoelectrochemical (PEC) hydrogen evolution from neutral aqueous electrolyte were performed with using the particulate photocathodes consisting of 40% Cu-excessive $(ZnSe)_{0.85}(CIGS)_{0.15}$ synthesized with various calcination times, 10—80 h, under intermittent irradiation of simulated sunlight, as compiled in Fig. S3. All Pt/CdS/$(ZnSe)_{0.85}(CIGS)_{0.15}$/Mo/Ti photocathodes prepared by the particle transfer (PT) method showed cathodic photocurrent from approximately 0.55—0.66 V_{RHE}, accompanied with anodic dark current at positive potential over ~0.6 V_{RHE}. Among the present photocathodes, $(ZnSe)_{0.85}(CIGS)_{0.15}$ synthesized for 15 h showed the highest cathodic photocurrent, approximately -2.5 mA cm^{-2} at 0 V_{RHE}. It should be noted that

$(ZnSe)_{0.85}(CIGS)_{0.15}$ particles in the previous report were synthesized for only 10 h.[1] The decreased cathodic photocurrent in the photocathodes consisting of $(ZnSe)_{0.85}(CIGS)_{0.15}$ particles synthesized for long time, 40—80 h, may be attributed to the too large size of the $(ZnSe)_{0.85}(CIGS)_{0.15}$ particles (see Fig. S2). Therefore, it can be concluded that 15 h of synthesis time should be optimal in the present case.

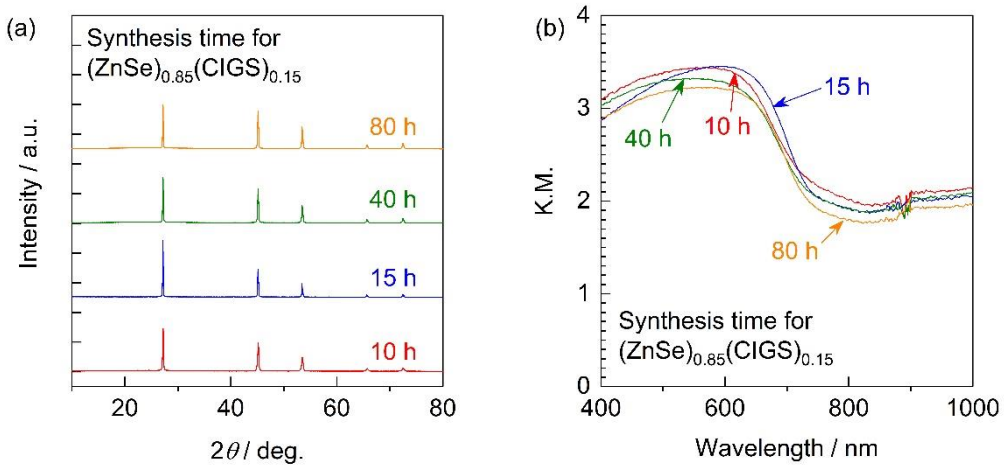

Fig. S1 (a) XRD patterns and (b) DRS spectra for Cu 40% excessive $(ZnSe)_{0.85}(CIGS)_{0.15}$ particles synthesized by the flux method for different calcination time, 10, 15, 40, and 80 h.

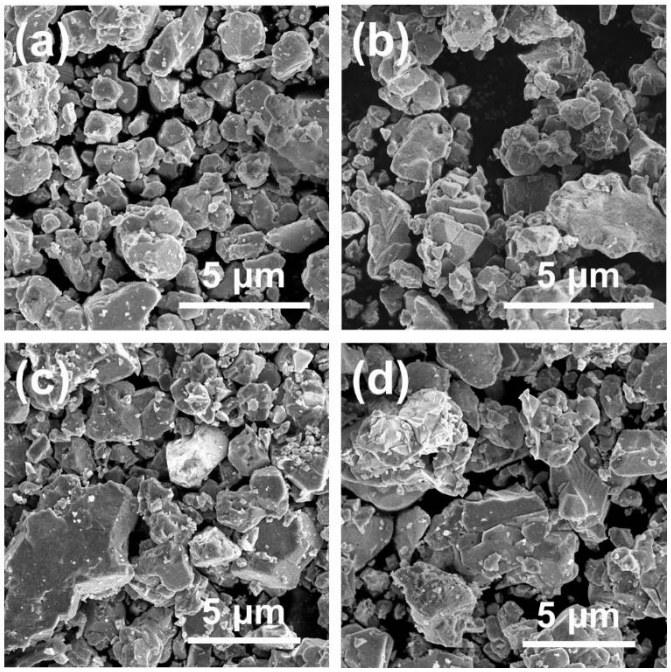

Fig. S2 SEM images for Cu 40%-excessive $(ZnSe)_{0.85}(CIGS)_{0.15}$ particles calcined for (a) 10, (b) 15, (c) 40, and (d) 80 h. Scale: 5 μm.

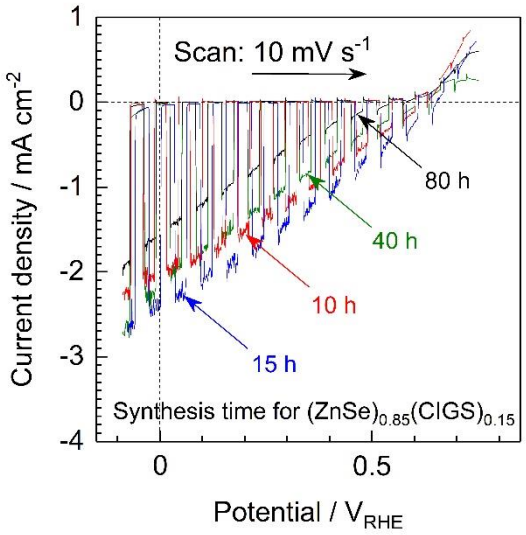

Fig. S3 Current-potential curves for Pt/CdS/$(ZnSe)_{0.85}(CIGS)_{0.15}$/Mo/Ti photocathodes consisting of Cu 40%-excessive $(ZnSe)_{0.85}(CIGS)_{0.15}$ particles synthesized with various calcination times, 10, 15, 40, and 80 h. Electrolyte: 1 M KPi (pH = 7). Light source: simulated sunlight (AM 1.5G)

Influence of thickness of Mo or C contact layer on the photoelectrochemical performances

The PEC hydrogen evolution from water was performed by the particulate $(ZnSe)_{0.85}(CIGS)_{0.15}$ photocathodes with various thicknesses of Mo contact layer under simulated sunlight (see Fig. S4) to elucidate the influence of thickness of Mo contact layer on the anodic dark current. Here, $(ZnSe)_{0.85}(CIGS)_{0.15}$ particles synthesized for 10 h, which is the same condition to the previous paper,[1] were used to prepare the photocathode. The deposition rate of Mo by the sputtering method was approximately 14.8 nm min^{-1}. Thus, Mo contact layers noted as 1, 2.5, and 5 min in Fig. S4 correspond to 14.8, 37.0, and 74.0 nm of nominal thickness, respectively. It should be noted that the typical $(ZnSe)_{0.85}(CIGS)_{0.15}$ photocathodes, as used in the previous paper[1] and body of the present paper, were prepared with Mo contact layer deposited for 5 min.

The $(ZnSe)_{0.85}(CIGS)_{0.15}$ photocathodes with Mo contact layer deposited for 2.5 and 5 min showed almost same cathodic photocurrent, -2.5 mA cm^{-2} at 0 V_{RHE}, while anodic dark current at positive potential, at >0.6 V_{RHE}, was obviously suppressed in the case of thinner Mo layer. Moreover, the photocathode with Mo contact layer deposited for only 1 min showed negligible anodic dark current at ~0.8 V_{RHE}. These experimental observations should also support that the anodic dark current at positive potential is caused by the oxidation of Mo-species in the backside electrode. However, the onset potential of the photocathode with Mo contact layer deposited for only 1 min

negatively shifted to around 0.6 V_{RHE} in spite of suppressed anodic dark current, and its cathodic photocurrent was also reduced less than -2 mA cm^{-2} at 0 V_{RHE}. The deteriorated PEC performances of the photocathode with the thinnest Mo contact layer should be attributed to partial contact between $(ZnSe)_{0.85}(CIGS)_{0.15}$ particles and Ti conductor layer, resulting in the formation of Schottky barrier. In addition, although thinner Mo layer certainly contributed to the suppression of anodic dark current at positive potential, there still remains non-negligible dark current even in the case of Mo layer deposited for 2.5 min. Thus, C contact layer and Mo/C bilayer contact were applied to further suppress the anodic dark current.

In our previous paper,[1] it was found that the use of C contact layer instead of Mo could suppress the anodic dark current at positive potential, resulting in the relatively positive onset potential. However, the cathodic photocurrent at negative potential was reduced compared to the case of Mo contact layer. Since the effects of the deposition conditions of C layer in the present PT photocathodes have not been investigated in detail, the thickness of C contact layer was optimized in this section. Here, the PEC performances of the particulate $(ZnSe)_{0.85}(CIGS)_{0.15}$ photocathodes with C contact layer deposited by the sputtering method for various times were assessed as shown in Fig. S5. The deposition rate of C was 1.3 nm min^{-1}. Therefore, C contact layers noted as 1, 5, 10, and 50 min in Fig. S5 correspond to 1.3, 6.5, 13, and 65 nm of nominal thickness, respectively. The photocathode with C contact layer showed negligible anodic dark current at ~0.8 V_{RHE}, compared with the case of Mo contact layer, resulting in the positive shift of the onset potential. Especially, the photocathode with C contact layer deposited for 5 min showed the most positive onset potential and comparable cathodic photocurrent to the case of Mo contact layer. In the case of C contact layer deposited for 1 min, slightly larger anodic dark current was observed than the case of thicker C layer (see Fig. S5b). This anodic dark current in C contact layer deposited for 1 min may be attributed to oxidation of exposed Ti conductor layer, implying the insufficient contact between $(ZnSe)_{0.85}(CIGS)_{0.15}$ particles and C layer. In other words, $(ZnSe)_{0.85}(CIGS)_{0.15}$ particles were partially contacted to Ti conductor layer, resulting in the formation of partial Shottky contact. On the other hand, the $(ZnSe)_{0.85}(CIGS)_{0.15}$ photocathodes with only C layer showed drastically reduced cathodic photocurrent, compared to the other cases. This is considered to be caused by the fragile feature of C layer and resultant loss of photocatalytic particles during electrode fabrication process. As shown in the top-view SEM images for the $(ZnSe)_{0.85}(CIGS)_{0.15}$ photocathode with various thicknesses of C back contact (see Fig. S6), cracks were observed at the surface of $(ZnSe)_{0.85}(CIGS)_{0.15}$ photocathodes with only C back contact, indicating disconnection of the in-plane electrical conductivity. In contrast, the surface of $(ZnSe)_{0.85}(CIGS)_{0.15}$/C/Ti with 5 min deposited C contact layer and subsequent Ti conductor layer was covered by the photocatalytic particles uniformly without obvious cracks. Therefore, it can be concluded that the C contact layer deposited for 5 min should be optimal to suppress the anodic dark current at positive potential and to achieve large cathodic photocurrent.

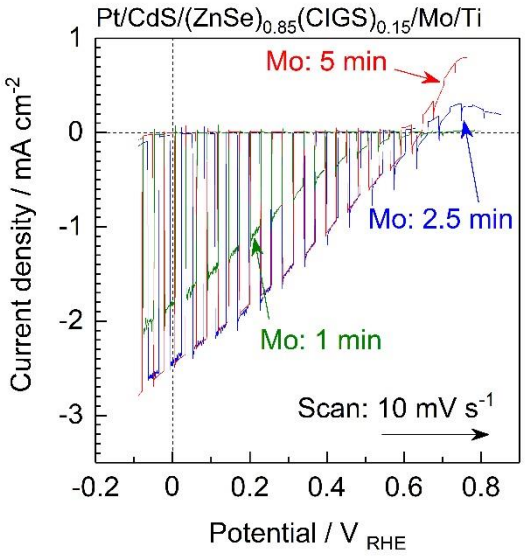

Fig. S4 Current-potential curves for Pt/CdS/$(ZnSe)_{0.85}(CIGS)_{0.15}$/Mo/Ti photocathodes prepared by the PT method with various thicknesses of Mo contact layer. The deposition rate of Mo by the sputtering method was approximately 14.8 nm min^{-1}. Electrolyte: 1 M KPi (pH = 7). Light source: simulated sunlight (AM1.5G)

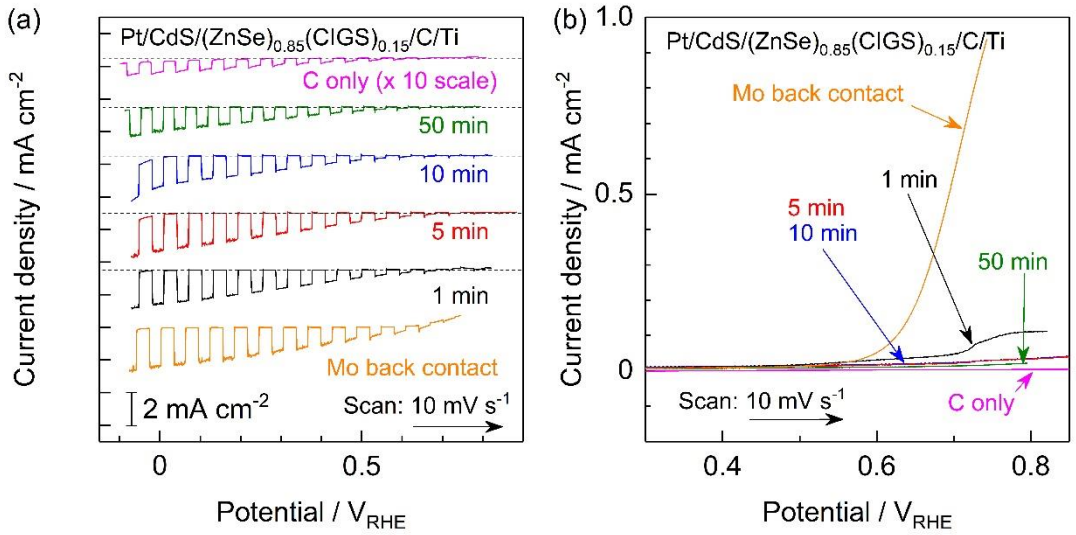

Fig. S5 Current-potential curves for Pt/CdS/$(ZnSe)_{0.85}(CIGS)_{0.15}$/C/Ti photocathodes prepared by the PT method with various thicknesses of C contact layer (a) under intermittent light irradiation and (b) under dark condition. The deposition rate of C by the sputtering method was approximately 1.3 nm min^{-1}. Electrolyte: 1 M KPi (pH = 7). Light source: simulated sunlight (AM1.5G)

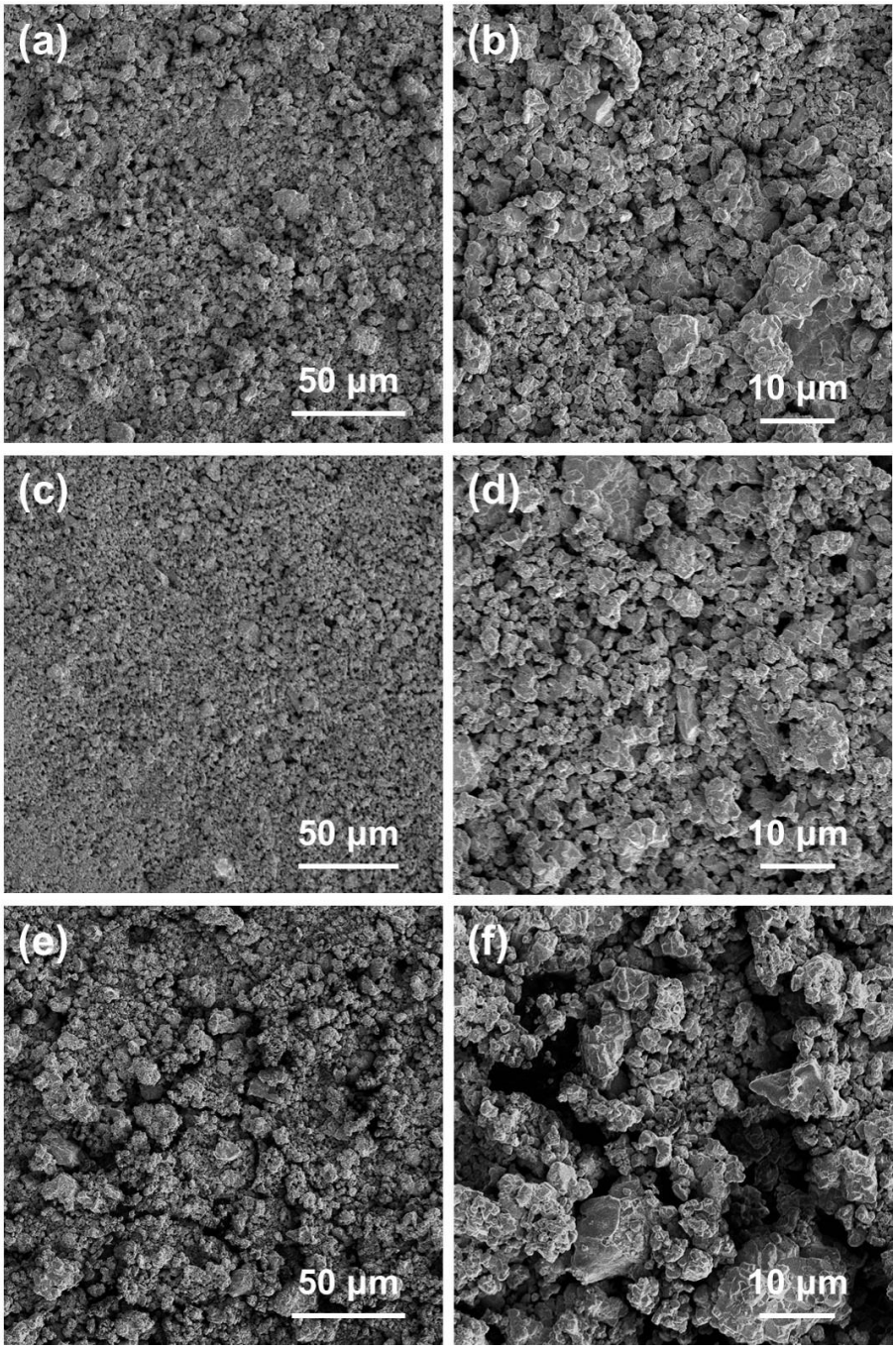

Fig. S6 Top-view SEM images of $(ZnSe)_{0.85}(CIGS)_{0.15}$/C/Ti photocathodes prepared with various thicknesses of C back contact layer. C layer was deposited for (a and b) 5 and (c and d) 50 min. (e and f) Only C layer was deposited as a backside electrode.

Effects of amount of Na_2S additive to the photoelectrochemical properties of stoichiometric and Cu 40%-excessive $(ZnSe)_{0.85}(CuIn_{0.7}Ga_{0.3}Se_2)_{0.15}$

The DRS spectra and XRD patterns of the stoichiometric $(ZnSe)_{0.85}(CIGS)_{0.15}$ synthesized with using various amounts of Na_2S additive were compared in Fig. S7. All diffraction peaks in the XRD patterns (see Fig. S7a) can be assigned to a zincblende phase without obvious impurities. All specimens showed clear absorption edge around 750—800 nm and weak light absorption at longer wavelength region over the absorption edge. The stoichiometric $(ZnSe)_{0.85}(CIGS)_{0.15}$ synthesized with overly large quantity of Na_2S (Na/Cu = 1) showed slightly blue-shifted absorption edge at around 700 nm, possibly due to partial incorporation of S species. The SEM images of the $(ZnSe)_{0.85}(CIGS)_{0.15}$ particles synthesized with stoichiometric Cu precursor and various amounts of Na_2S additive are displayed in Fig. S8. The stoichiometric $(ZnSe)_{0.85}(CIGS)_{0.15}$ synthesized without Na_2S possessed an indefinite and rugged shape, while the solid solutions synthesized with Na_2S additive showed clear triangle-shaped crystal, regardless of the added amount of Na_2S. The particle size of the $(ZnSe)_{0.85}(CIGS)_{0.15}$ distributed widely in the range of submicron to micron-order.

According to increased amount of added Na_2S during synthesis, the cathodic photocurrent of the stoichiometric $(ZnSe)_{0.85}(CIGS)_{0.15}$ photocathodes was drastically improved and gradually decreased with overly large quantity of the additive, resulting in the highest photocurrent in the case of Na/Cu = 0.2 (see Fig. S9). It should be noted that the optimal photocathode consisting of the stoichiometric $(ZnSe)_{0.85}(CIGS)_{0.15}$ synthesized with Na/Cu = 0.2 of Na_2S showed as much as two times higher cathodic photocurrent at negative potential, approximately -4 mA cm^{-2} at 0 V_{RHE}, than the conventional one, as discussed in the main body of this paper.

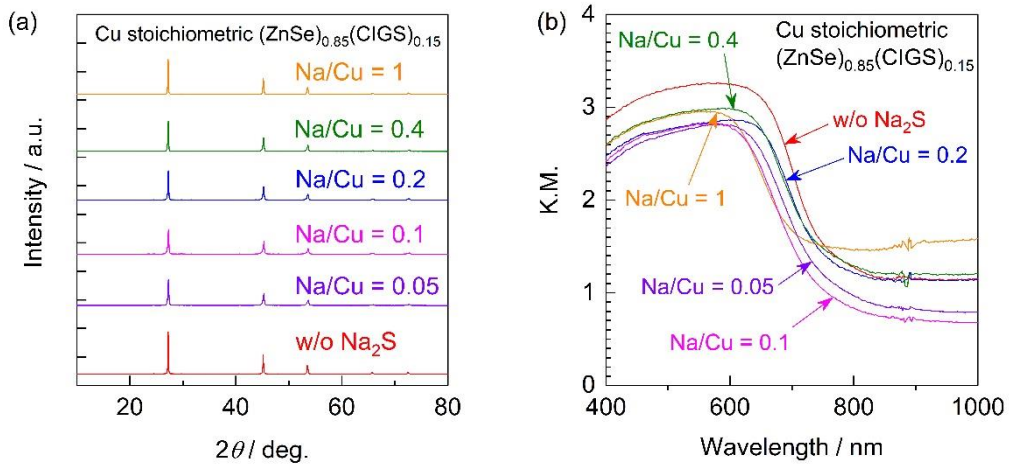

Fig. S7 (a) XRD patterns and (b) DRS spectra for stoichiometric $(ZnSe)_{0.85}(CIGS)_{0.15}$ particles synthesized with various amounts of Na_2S additive. Na/Cu = 0, 0.05, 0.1, 0.2, 0.4, and 1.

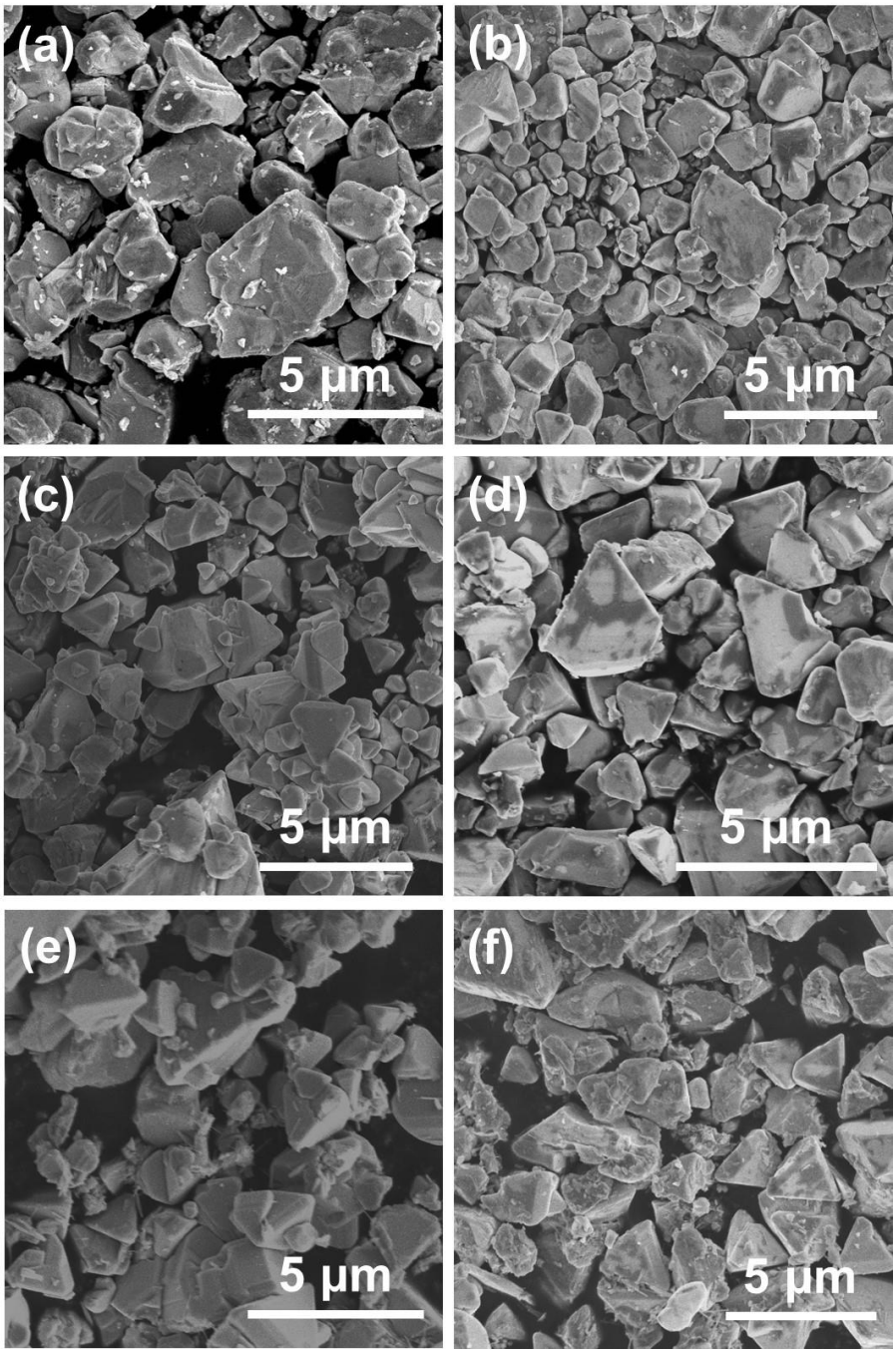

Fig. S8 SEM images for the stoichiometric $(ZnSe)_{0.85}(CIGS)_{0.15}$ particles synthesized with various amounts of Na_2S additive, Na/Cu = (a) 0, (b) 0.05, (c) 0.1, (d) 0.2, (e) 0.4, and (f) 1.

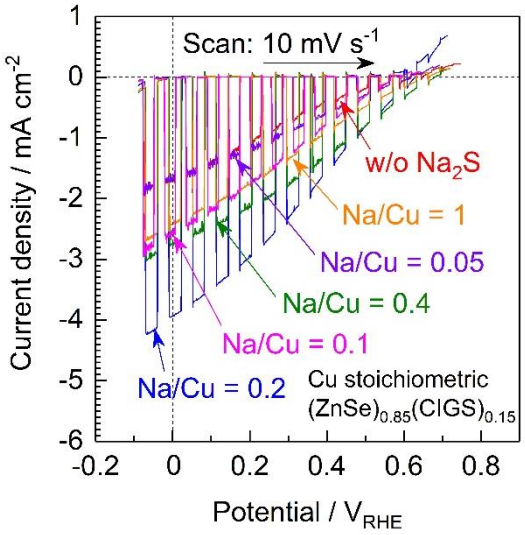

Fig. S9 Current-potential curves for Pt/CdS/$(ZnSe)_{0.85}(CIGS)_{0.15}$/Mo/Ti photocathodes. The photocatalytic particles were synthesized under Cu stoichiometric condition with using various amounts of Na_2S additive (Na/Cu = 0.05—1). Electrolyte: 1 M KPi (pH = 7). Light source: simulated sunlight (AM1.5G)

In order to confirm the effects of Na_2S additive in more detail, the Cu 40%-excessive $(ZnSe)_{0.85}(CIGS)_{0.15}$ were also synthesized with using Na_2S additive, such that the molar ratio was Na/(In + Ga) = 0.2—0.4. The XRD patterns, DRS spectra, and SEM images of the specimens were displayed in Fig. S10 and 11, while the current-potential curves were also compiled in Fig. S12. They showed similar tendencies to the case of the stoichiometric $(ZnSe)_{0.85}(CIGS)_{0.15}$ synthesized with Na_2S.

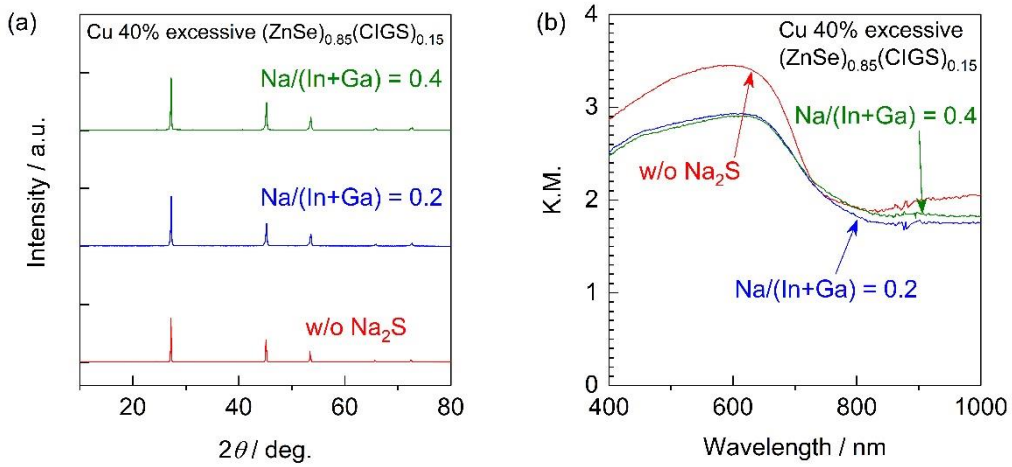

Fig. S10 (a) XRD patterns and (b) DRS spectra for Cu 40%-excessive $(ZnSe)_{0.85}(CIGS)_{0.15}$ particles synthesized with various amounts of Na_2S additive. Na/Cu = 0, 0.2, and 0.4.

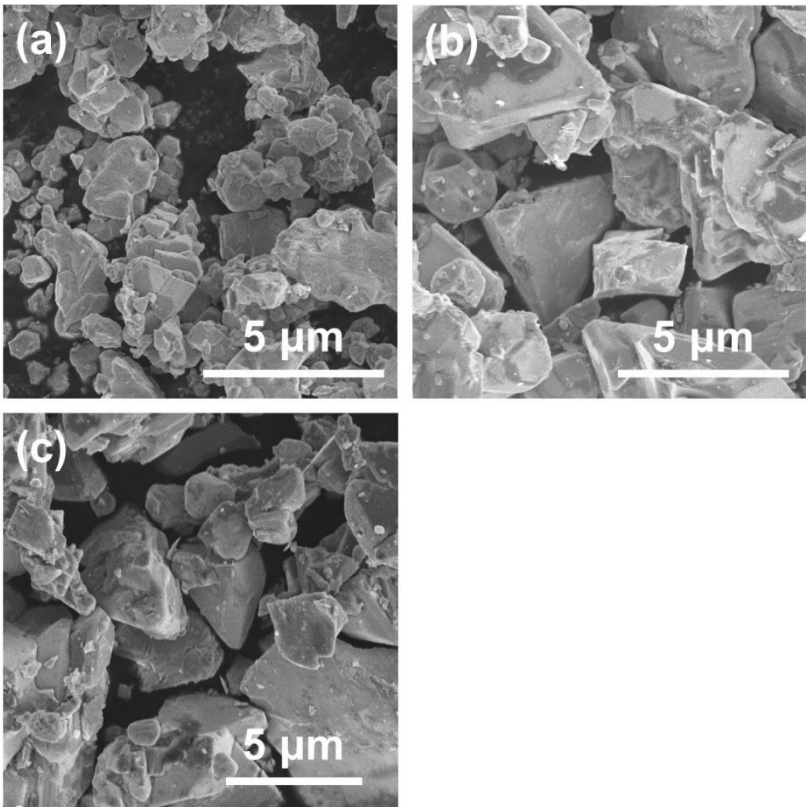

Fig. S11 SEM images for the Cu 40%-excessive $(ZnSe)_{0.85}(CIGS)_{0.15}$ particles synthesized with various amount of Na_2S additive, Na/(In + Ga) = (a) 0, (b) 0.2, and (c) 0.4.

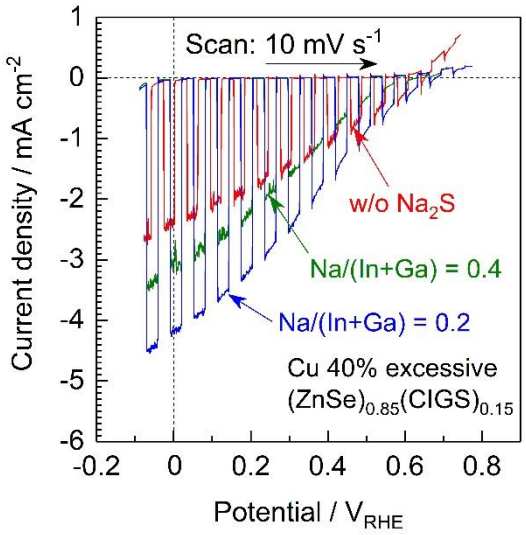

Fig. S12 Current-potential curves for Pt/CdS/$(ZnSe)_{0.85}(CIGS)_{0.15}$/Mo/Ti photocathodes. The photocatalytic particles were synthesized under Cu 40%-excessive condition with using various amounts of Na_2S additive (Na/(In + Ga) = 0.2 and 0.4). Electrolyte: 1 M KPi (pH = 7). Light source: simulated sunlight (AM1.5G)

Elemental composition analyses by ICP-MS

The elemental composition of the $(ZnSe)_{0.85}(CIGS)_{0.15}$ particles were determined by ICP-MS as described in the main body of this paper. Cu content in the Cu-deficient, stoichiometric, and Cu excessive $(ZnSe)_{0.85}(CIGS)_{0.15}$ determined by ICP-MS and calculated from the amounts of precursors were compiled in Fig. S13 as a function of the amount of Cu precursor, Cu/(In + Ga). In all cases of the amount of Cu precursor, actual Cu content in the solid solutions well agreed with the amount of precursor.

In addition, results of composition analyses for the samples synthesized with Cu 40%-excessive composition of precursors and different amounts of Na_2S additive were summarized in Fig. S14. The observed cation contents in the Cu 40%-excessive $(ZnSe)_{0.85}(CIGS)_{0.15}$ particles synthesized with various amounts of Na_2S showed the similar tendencies to that of stoichiometric $(ZnSe)_{0.85}(CIGS)_{0.15}$ synthesized with Na_2S additive, as discussed in Fig. 7b in the main body of this paper.

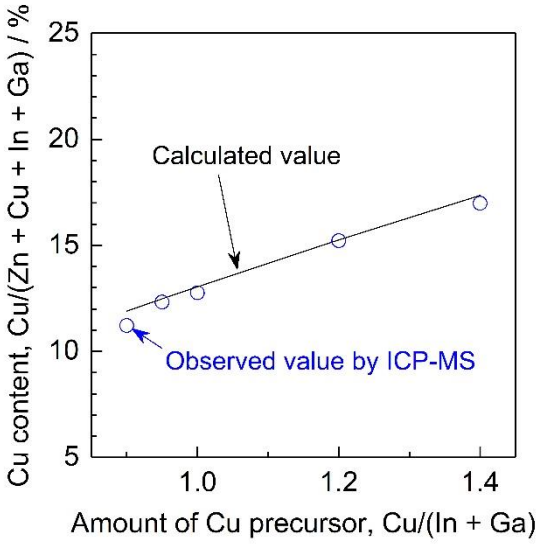

Fig. S13 Ratio of Cu in $(ZnSe)_{0.85}(CIGS)_{0.15}$ particles synthesized with various amounts of Cu precursor, Cu/(In + Ga) = 0.9—1.4, without Na_2S additive. Cu content, Cu/(Zn + Cu + In + Ga), were determined by ICP-MS (blue circles) and calculated from the amount of precursors (black solid line).

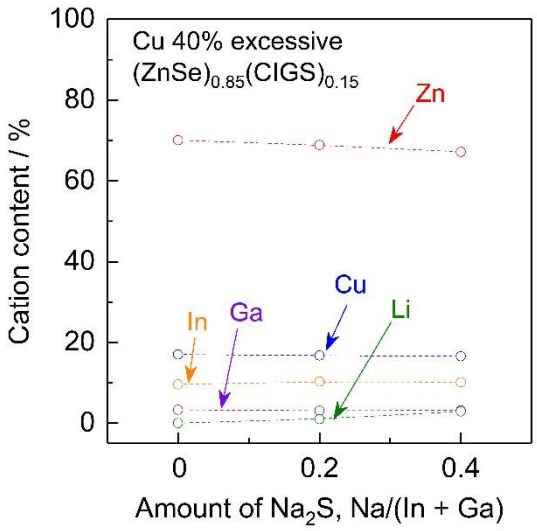

Fig. S14 Ratio of Zn, Cu, In, Ga, and Li in Cu 40%-excessive $(ZnSe)_{0.85}(CIGS)_{0.15}$ synthesized with various amounts of Na_2S additive, Na/Cu = 0—0.4. Cation contents indicate M/(Zn + Cu + In + Ga + Li), M = Zn, Cu, In, Ga, or Li.

Depth profiles of Cu, O, and Se at the surface of $(ZnSe)_{0.85}(CuIn_{0.7}Ga_{0.3}Se_2)_{0.15}$ photocathodes determined by XPS

The XPS analyses were conducted for the particulate $(ZnSe)_{0.85}(CIGS)_{0.15}$/Mo/Ti photocathode prepared by the PT method. The photocatalytic particles-metal layer assembly was fixed onto glass plate by carbon tape, followed by removing excessive particles by sonication and KCN etching as describe in the experimental section. Since the surface of the photocatalytic particles should be oxidized after exposed to air, surface of the photocathodes was etched by Ar ion sputtering until the peak area of O 1s was saturated. The typical XPS spectrum obtained from the particulate photocathode consisting of stoichiometric $(ZnSe)_{0.85}(CIGS)_{0.15}$ particles synthesized with Na_2S additive, Na/Cu = 0.2m, was shown in Fig. S15. The surface of the photocathode was etched by Ar ion sputtering for 200 nm-SiO_2 equivalent.

The depth profile of Cu 2p, O 1s, and Se 3d signals in the XPS spectra were summarized in Fig. S16. According to Ar ion sputtering, peak area of O 1s gradually decreased and almost saturated after 200 nm-SiO_2 equivalent etching, indicating that the remaining O 1s signal should reflect O atoms in the lattice rather than surface oxide. Peak area ratios of Cu 2p and Se 3d seemed unchanged after the Ar ion sputtering. It should be noted that O 1s signal derived from SLG substrate was also detected at high binding energy in the case of $(ZnSe)_{0.85}(CIGS)_{0.15}$ synthesized without Na_2S additive (see Fig. S16a), since the geometric surface area of the photocathode was smaller than the others were.

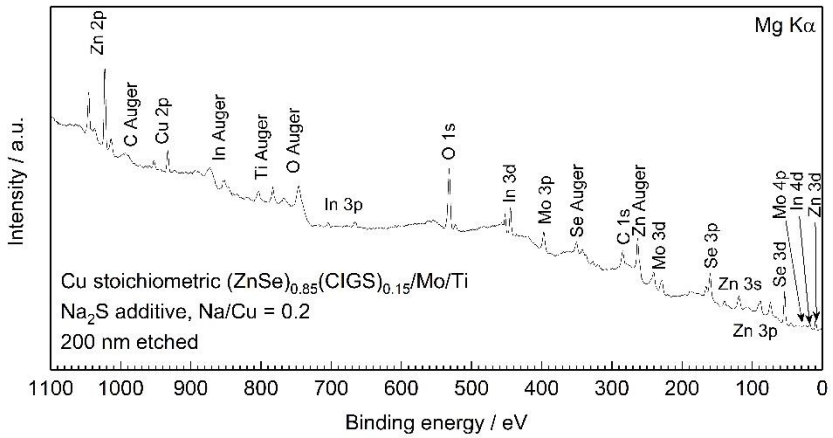

Fig. S15 XPS spectrum obtained from the particulate photocathode consisting of stoichiometric $(ZnSe)_{0.85}(CIGS)_{0.15}$ synthesized with Na_2S additive, Na/Cu = 0.2.

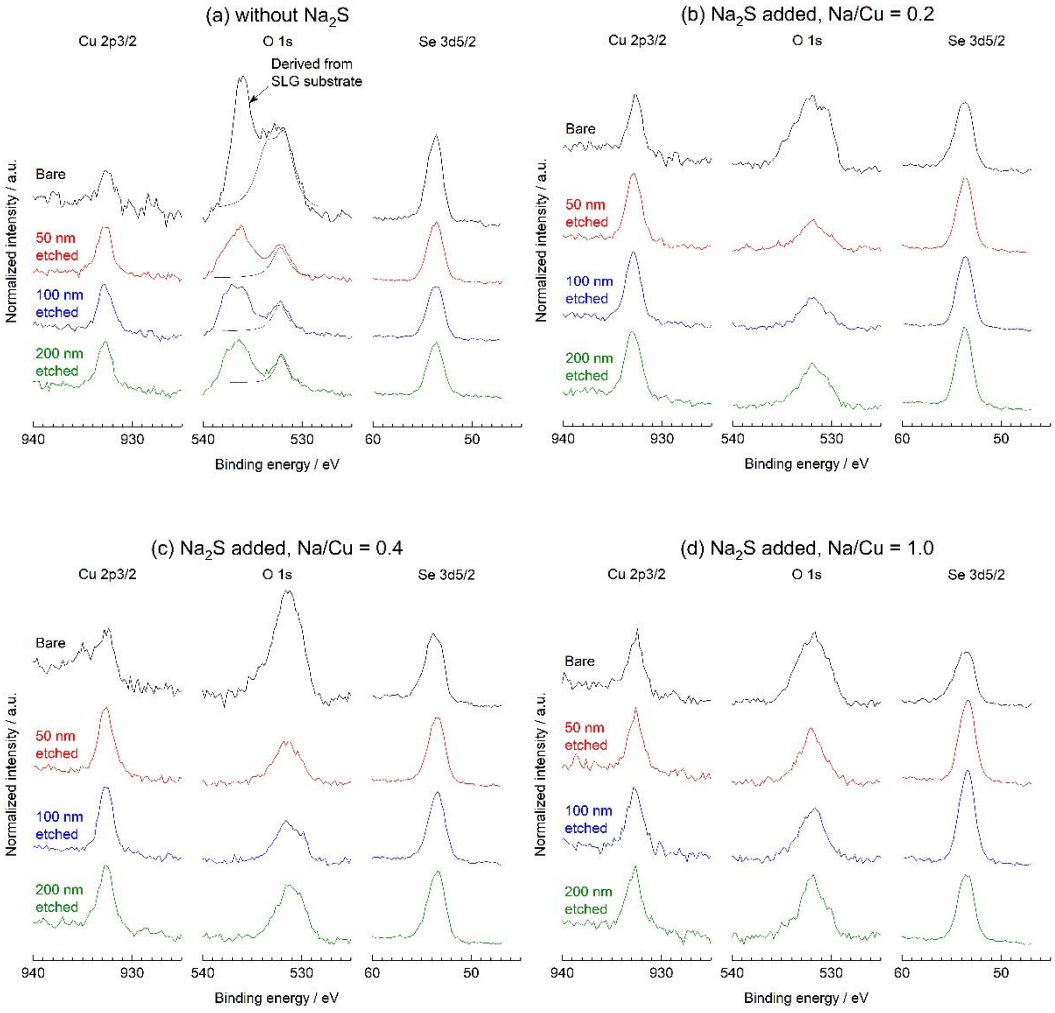

Fig. S16 Depth profiles for Cu2p, O 1s, and Se 3d signals in the XPS spectra.

Product analysis for the photoelectrochemical water splitting reaction

To confirm the faradaic efficiencies for hydrogen evolution by the present $(ZnSe)_{0.85}(CIGS)_{0.15}$ photocathodes, product analysis was conducted by using Pt/ZnS/CdS/$(ZnSe)_{0.85}(CIGS)_{0.15}$/Mo/C/Ti as shown in Fig. S17. The PEC reaction was performed in batch type reactor connected to μGC. The amount of hydrogen and oxygen determined by μGC well agreed with the simultaneously recorded photocurrent, indicating that the faradaic efficiency for water splitting in the present PEC system was almost 100%.

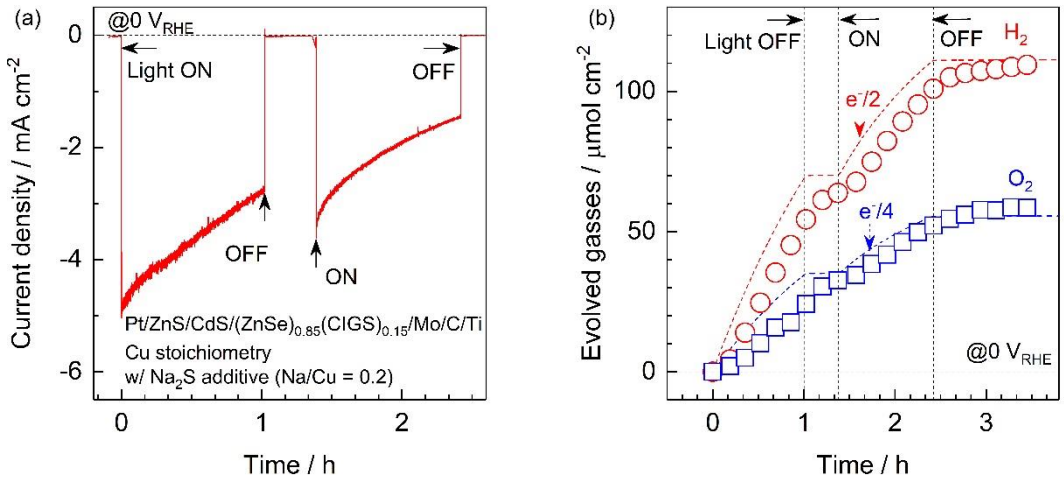

Fig. S17 Time courses for (a) photocurrent and (b) evolved hydrogen and oxygen during PEC water splitting with using Pt/ZnS/CdS/$(ZnSe)_{0.85}(CIGS)_{0.15}$/Mo/C/Ti photocathode. The photocatalytic particles were synthesized under Cu-stoichiometric condition and Na_2S additive. Electrolyte: 1 M KPi (pH = 7). Light source: simulated sunlight (AM 1.5G)

Reference

1. Y. Goto, T. Minegishi, Y. Kageshima, T. Higashi, H. Kaneko, Y. Kuang, M. Nakabayashi, N. Shibata, H. Ishihara, T. Hayashi, A. Kudo, T. Yamada and K. Domen, *J. Mater. Chem. A*, 2017, **5**, 21242-21248.